ELEMENTAL EVIDENCE FOR GLOBAL VOLCANOGENIC INPUT AT THE KPg BOUNDARY BASED ON RESULTS FROM EL KEF, TUNISIA. S. Sillitoe-Kukas[1], M. Humayun[1], T. Adatte[2], G. Keller[3], [1]National High Magnetic Field Laboratory and Department of Earth, Ocean & Atmospheric Science, Florida State University, Tallahassee, FL 32310, USA (sms17w@my.fsu.edu); [2]Institute of Earth Sciences (ISTE), University of Lausanne, Géopolis, CH-1015 Lausanne, Switzerland; [3]Department of Geosciences, Princeton University, Princeton, NJ 08544, USA.

Introduction: The Cretaceous-Paleogene (KPg) extinction occurred contemporaneously with Deccan Trap volcanism and the Chicxulub impact [1-5]. Several lines of evidence speak to major changes in elemental geochemical cycles of Ir [6], Os [5] and Hg [7], preceding or during the KPg boundary event, but uniquely assigning these changes to volcanism or impact has proved elusive [8]. Recent recognition that the KPg boundary is synchronous with the end of the Poladpur phase of Deccan volcanism [9] and the presence of ubiquitous Hg spikes in sediments preceding the KPg boundary indicate that volcanic emissions played a key role in the environmental change leading to the extinction [7]. Large eruptions release significant quantities of metals, metalloids and sulfur gases to the atmosphere, a majority of which are globally distributed [10, 11]. The recognition of high concentrations of Ir in volcanic aerosols raised the possibility of volcanism rather than impact being the source of siderophiles at the KPg boundary [12]. A quantitative assessment of the role of volcanism in contributing global siderophile element enrichment would require a knowledge of the emission rates for volcanoes from all major tectonic settings. Available data for siderophile emissions are limited to a few volcanic centers [13, 14].

To examine volcanogenic tracers from the Deccan eruption pulses in KPg sediments, we analyzed the El Kef KPg stratotype by laser ablation ICP-MS [15, 16]. We also re-examine the global KPg siderophile element distribution in the context of volcanogenic aerosol contributions to the boundary.

Analytical Methods: Polished sections of epoxy impregnated sediments taken from 3 cm above to 21 cm below the KPg boundary at El Kef were analyzed by LA-ICP-MS using an ESI™ New Wave™ UP193FX laser ablation system coupled to a Thermo Element XR™ at the Plasma Analytical Facility at FSU [15]. Samples were analyzed with line scans using 100 µm spot sizes and 50 Hz repetition rate. Standards used were GSD-1g, NIST SRM 610, pyrite, calcite, gypsum and the Hoba (IVB) iron meteorite.

Results: A chemical profile of the KPg boundary reveals three components: clay, gypsum and Fe-oxyhydroxides (goethite) [17]. Bulk Co, Ni and Ir concentrations in the El Kef boundary sediment are identical to those reported previously [18]. Siderophile enrichments are found in the goethite component of the boundary [16]. Osmium is enriched in the boundary relative to Ir, resulting in a super-chondritic Os/Ir ratio [16]. Samples above, on and below the KPg boundary at El Kef are enriched in Cd and Re. Boundary samples exhibit Cd/Re ratios comparable to those in volcanic aerosols outgassed from the Erta A'le volcano in Ethiopia (Fig. 1). Some El Kef sediments exhibit high enrichments of Re from other processes (Fig. 1). The $(Ru/Ir)_{CI}$ ratios measured by LA-ICP-MS were higher than reported for global KPg $(Ru/Ir)_{CI}$ [19] and might have been compromised by NiAr+ interferences, so are not shown in Fig. 2. The $(Pd/Ir)_{CI}$ ratios are super-chondritic even at high Ir concentrations (Fig. 2).

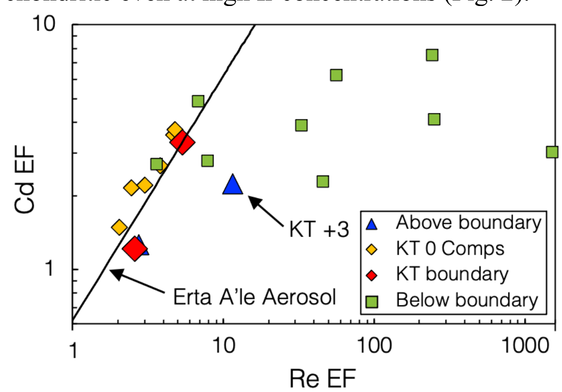

Fig. 1: Cd vs. Re enrichment factors (EF) relative to Upper Continental Crust (UCC) [20] in the KPg sediments at El Kef. The black line represents mixing between Erta A'le aerosols [12] and UCC [19]. KT 0 Comps represent the individual components in the boundary clay [16].

Discussion: Differentiating volcanic aerosols and chondritic contamination in sediments is crucial for determining the cause of the KPg extinction. When Erta A'le composition [13] aerosol is mixed with sediment, approximated by the upper continental crust (UCC) [20], the order by which the enrichment of trace metals occurs is Re>Cd>Os>Ir. Osmium is a highly siderophile element (HSE) that is abundant in chondrites and due to its volatile nature in oxidized environments is outgassed readily, condensing in volcanic aerosols. The chondritic Os/Ir ratio is ~1 [5] but the KPg boundary at El Kef is super-chondritic [16], a feature of volcanic aerosol deposition, not chondritic influx, where the Os/Ir ratio is ~1. The Enrichment Factor (EF) is defined as the concentration of a metal in the sediment + aerosol mix relative to that of UCC. The EFs for Cd and Re observed for El Kef sediments coincidentally plot on the trend for Erta A'le (Fig. 1). Sediment analyzed 3 cm above the boundary at El Kef shows little enrichment in Cd or Re, interpreted here as being deposited between the Poladpur and Ambenali eruptions.

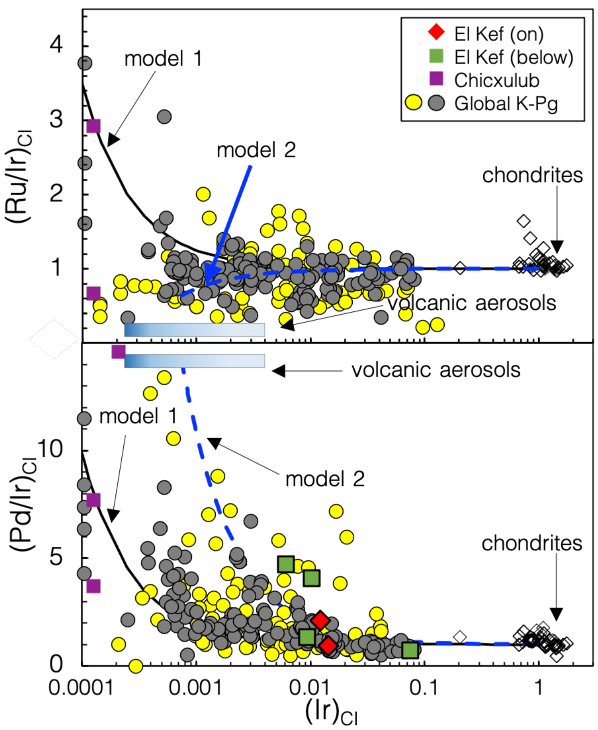

Fig. 2: Siderophile element ratios for global KPg sediments compared with El Kef KPg sediments [19, 21, 22], Chicxulub impactites [23] and chondrites [24]. Model 1 (solid line) represents mixing of UCC [20] with chondrites [24]. Model 2 (dashed line) represents UCC to which volcanic aerosol [14] was added to increase Ir ten-fold followed by chondritic addition. Mixtures of UCC with volcanic aerosols are shown as blue bars.

There is a dearth of coverage of siderophile element concentrations in volcanic emission but what data exists indicates that siderophile element patterns are similar to basaltic siderophile element patterns [13,14]. Relative emission rates of Ru were found to be lower than those of Ir for the Kudryavy volcano, while those of Pd were found to be higher [14]. To examine whether a global signature of volcanic emissions can be discerned in KPg sediments, we made mixing models for UCC, chondrites and volcanic aerosols and compared these with KPg sediments [6, 19, 21, 22].

An impact model requires that mixing occur between the chondritic endmember and UCC, shown as Model 1 in Fig. 2. Neither the $(Ru/Ir)_{CI}$ nor the $(Pd/Ir)_{CI}$ ratios for the global KPg sites plot along Model 1 curves (Fig. 2). When volcanic aerosols are arbitrarily added to UCC and the resulting mixture then admixed with CI chondrite the result is Model 2. The crustal end members then have sub-chondritic $(Ru/Ir)_{CI}$ and super-chondritic $(Pd/Ir)_{CI}$, which when mixed with chondritic material could explain global KPg sediment compositions (Fig. 2). The global KPg sites [6, 19] appear to require volcanic aerosol input dominating certain siderophile element ratios (Fig. 2). The chemical features noted above are not specific to a single site and are witnessed widely along the KPg boundary. This argues against local volcanic inputs and in favor of Deccan emissions. The Kudryavy volcano is an arc volcano [14], and hotspot and arc metal emissions are distinct for many elements [10]. If Deccan emissions share the sub-chondritic Ru/Ir ratios of emissions from the Kudryavy volcano, then the sub-chondritic Ru/Ir ratio (Fig. 2) indicates that much of the siderophile inventory at global KPg sites may have been sourced from Deccan aerosols. In view of this, once more relevant metal emission rates are available a thorough assessment of the role of volcanoes in siderophile element enrichment is warranted.

References: [1] Alvarez L.W. et al. (1980) *Science 208*, 1095-1108. [2] Courtillot V. et al. (2000) *EPSL 182*, 137-156. [3] Officer C.B. and Drake C.L. (1983) *Science 219*, 1383-1390. [4] Keller G. et al. (1995) *PPP 119*, 221-254. [5] Ravizza G. et al. (2003) *Science 302*, 1392-1395. [6] Lee C-T A. et al. (2003) *GCA 67*, 655-670. [7] Keller G. et al. (2020) *GPC 194*, 103312. [8] Ravizza G. et al (2012) *Paleoceanography 27 PA3219*. [9] Schoene B. et al. (2019) *Science 363*, 862-866. [10] Edmonds M. et al. (2018) *Nature Geosci. 11*, 790-794. [11] Self S. et al. (2014) *GSA SP505*. [12] Toutain J.-P. and Meyer G. (1989) *GRL 16*, 1391-1394. [13] Zelenski M.E. (2013) *Chem. Geol. 357*, 95-116. [14] Yudovskaya M.A. et al. (2008) *Chem. Geol. 249*, 318-341. [15] Yang S. et al. (2018) *G-cubed 19*, 4236-4259. [16] Sillitoe-Kukas S. et al. (2020) LPSC abstract# 1111. [17] Adatte T. et al. (2002) *PPP 2754*, 1-32. [18] Meyer G. et al. (1993) *J. Radioanalyt. Nuc. Chem. 168*, 125-131. [19] Goderis S. et al. (2013) *GCA 120*, 417-446. [20] Rudnick R.L. and Gao S. (2003) Treatise on Geochemistry. [21] Evans N. J. et al. (1994) *MaPS 29*, 223-235. [22] Evans N.J. et al. (1995) *EPSL 134*, 141-153. [23] Tagle R. et al. (2004) *MaPS 39*, 1009-1016. [24] Fischer-Gödde M. et al. (2010) *GCA 74*, 356-379.